Evaluation on the Performance of Cross-Matrix Absorber Double-Pass Solar Air Heater (CMA-DPSAH) with and without Thermal Energy Storage Material

Open Access

Ahmad Fadzil Sharol[1], Amir Abdul Razak[1,*], Zafri Azran Abdul Majid[2], Muhammad Amirul Azwan Azmi[1], Muhammad Amir Syahiran Muhammad Tarminzi[1]

[1] Energy Sustainability Focus Group (ESFG), Faculty of Mechanical and Automotive Engineering, Universiti Malaysia Pahang, 26600 Pekan, Pahang, Malaysia
[2] Kuliyyah of Allied Health and Sciences, International Islamic University of Malaysia, 25200 Kuantan, Pahang, Malaysia

ARTICLE INFO	ABSTRACT
	The intermittent nature of solar energy source can reduce the performance of solar air heater (SAH) considerably. The utilization of thermal storage materials demonstrates an effective way in order to improve an overall performance of SAH. In the present study, the performance of cross-matrix absorber double-pass solar air heater (CMA-DPSAH) integrated with the phase change material (PCM) as thermal energy storage was conducted. The PCM material was inserted inside the rectangular aluminium tube used as the thermal absorber. The air mass flow rate of 0.004 kg/s was used during the entire experimental period. The experiment was conducted on several phase; Phase 1 (CMA-DPSAH with PCM) and Phase 2 (CMA-DPSAH without PCM) in order to compare and evaluate the effectiveness of the PCM utilization. Based on the result, CMA-DPSAH with PCM performed better than the CMA-DPSAH without PCM with maximum of heat gain and temperature output were 127 W and 53 °C, respectively. The instantaneous efficiency of CMA-DPSAH with PCM consistently higher than the CMA-DPSAH without PCM for about 17 – 19% with the maximum was 64 % during the low radiation flux. This feature offers a great potential of solar air heater application in the intermittent solar radiation condition, especially for drying of the agriculture products.

1. Introduction

Solar engineering technology was going through a great technological advancement in terms of the design configuration of the solar collector in the past decades. In the application of solar air

---

heater (SAH), there were a lot of innovative design of the solar energy harvesting devices have been highlighted in the literature in order to maximize the rate of heat transfer from the surface of thermal absorber to the flowing heat transfer fluid [1]. These advancement including the utilization of finned thermal absorber surfaces [2-4], insertion of porous structure [5-7] and the implementation of artificial roughness on the thermal absorber surface [8-10] and the execution of multiple pass of heat transfer fluid (air) [10-12]. However with the intermittent nature of solar energy source [13-14], making the SAH difficult to achieve a better overall efficiency and limiting its operating time. The incorporation of thermal energy storage material into the solar energy system has been seen as a suitable and practical solution in order to maximize the utilization of solar thermal devices in the situation of intermittent solar radiation and/or during off-sunshine period.

From literature, there have been increasing trends on the study related to the integrated SAH with the thermal energy storage system in order to increase the performance of the solar air heater. Some study using sensible energy storage material in order to stock the thermal energy during the peak hours [15]. However, the major drawback of the sensible energy storage material is that they require a relatively huge size of material in order to increase the rate of energy stored [16]. As compared to sensible energy storage material, latent energy storage material in the form of phase change material (PCM) have a higher energy storage to mass ratio and energy can be stored within the narrow range of operating temperature [17-19], making them most favorable type of energy storage material in the application of solar air heaters. Bouadilla *et al.,* [20] has conducted an experimental investigation about the SAH integrated with packed-bed of spherical capsules of SN27 material as the thermal energy storage materials. The spherical capsules were built from a blend of polyolefin and was painted with flat black in order to act as the thermal absorber component of the SAH. Based on their study, it was concluded that the SAH system managed to supply an amount of useful heat of 200 W/m^2 for an extended period of time after the off-sunshine period. Double-pass solar air heater (DPSAH) integrated with rectangular capsules of paraffin wax was investigated by Salih *et al.,* [21]. The experimental work was conducted to evaluate the DPSAH thermal efficiency with the variation of solar radiation and mass flow rate. The numerical study was also conducted with the result from the developed mathematical model agreed well with the experimental result. Baig and Ali [22] investigated the effect of using the aluminum foam embedded in the PCM duct located on the top of the thermal absorber of DPSAH. The configuration was compared with the DPSAH having a similar arrangement but with no aluminum foam insertion. They concluded that the insertion of aluminum foam material was increase the PCM conductivity but reduce its thermal storage capability with useful heat gain time was 30 minutes faster than the one without aluminum foam insertion. The comparison between paraffin wax and carbon granular powder have been investigated by Saxena *et al.,* [23]. The experimental comparison was carried out based on natural and forced convection mode with the energy storage materials were inserted inside the copper cylinder tubes in order to investigate the influence of heat transfer coefficient of the air heater. The extend of the investigation also reach to the stage where both materials (paraffin wax and carbon granular powder) were combined as a heat storage material for the investigated air heated. Based on the experimental result, it was concluded that the air heater with combination of energy storage material provided the highest efficiency of 78.31% and capable of supplying the moderate air temperature to the consumer up into the extended hours.

Comparison between rectangular and cylindrical shape of PCM encapsulation was conducted experimentally by A.K. Raj *et al.,* [24]. The PCM encapsulations were located on the top side of thermal absorber in order to investigate the thermal efficiency of both DPSAH configurations. According to the studies, they concluded that the rectangular encapsulation provides thermal storage efficiency of 67 % as compared to the cylindrical encapsulation of 47.2 %. This was due to the

fact that during the rectangular encapsulation mode, the temperature different between the thermal absorber and the bottom plate is higher, which mean that the absorption of radiation flux was higher than the cylindrical encapsulation mode. The indoor experimental investigation of integrated zig-zag configuration of cross-matrix absorber in single-pass solar air heater (SPSAH) has been conducted by Sharol *et al.,* [25] by varying the input parameters of mass flow rate and solar radiation. Based on the result, it is concluded that the output temperature and heat gain were directly and indirectly proportional to the mass flow rate, respectively. From the recent literature studies conducted, it is evidence that the incorporation of thermal energy storage material into the SAH system plays a significant role in order to improve the thermal efficiency of the SAH and prolonged the operation of the air heater itself. The objective of current study is to investigate the performance of a new design of double-pass solar air heater (DPSAH) with cross-matrix thermal absorber arrangement integrated with paraffin wax as a latent heat energy storage material experimentally. Based on author knowledge, there was no similar study conducted on the integration of thermal storage material inside the rectangular aluminum tube arranged in the cross-matrix arrangement inside the double-pass air heater.

2. Description of CMA-DPSAH

The schematic diagram of the CMA-DPSAH as shown in Figure 1 was constructed using the locally available materials. The device consists of a set of collectors made of polypropylene having a dimension of 525 mm length, 400 mm width and 180 mm height. The CMA-DPSAH was built from polycarbonate transparent cover, intermediate polycarbonate transparent cover, and set of rectangular aluminium tubes act as an absorber. The rectangular aluminium tube comprises of two types of aluminium tube namely; type A (326 mm Length, 19.1 mm width, 19.1 height and 1 mm thickness) which was positioned perpendicular to the air flow and type B (427 mm Length, 19.1 mm width, 19.1 height and 1 mm thickness) which was positioned parallel with the air flow. The spacers were located at the bottom absorber of each pass in order to avoid direct contact to the bottom wall of the absorber and surface of the intermediate glazing plate. The tubes were sprayed with flat black coating and arranged in a staging manner in order to increase the heat absorption and to optimize the aperture area of the tubes [26], respectively. The total aperture area of the thermal absorber was calculated to be 0.3786 m^2. The 6 mm thickness of insulation sheet was applied at the edge and bottom side of the collector in order to reduce the heat losses. Three units of brushless 24 V DC fan were installed at the outlet chamber of the collector in order to force the outdoor air into the air passage of the collector. The incoming air entered to the first pass of the collector through the three identical circle shape inlet duct before went to the second pass through 3.3 cm diameter flexible hose. Figure 2 shows the experimental setup used in this work.

Additionally, paraffin wax in the form of granulated particle was inserted in the tube type B and was sealed with rubber cap to prevent from leaking. The thermophysical properties of the paraffin wax is shown in Table 1.

Table 1
Thermophysical properties of paraffin wax used in this study [27]

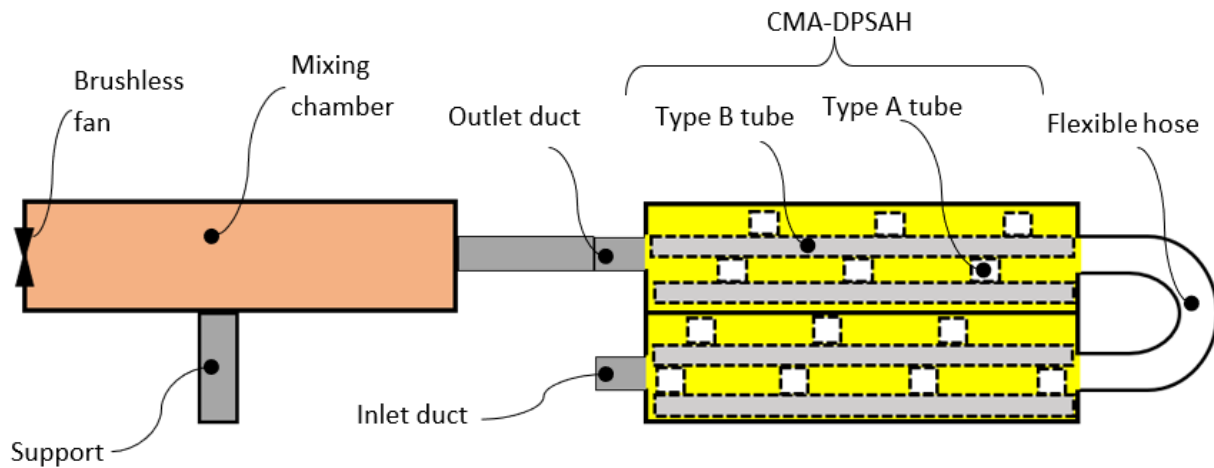| Properties	Value
Melting temperature, T_m (°C)	58 - 60
Specific heat (solid), $C_{P,s}$ (J/kg.K)	900
Enthalpy of fusion, L_f (kJ/kg)	214.4
Total weight (g)	624

Fig. 1. Schematic diagram of the CMA-DPSAH system

2.1 Description of Experimental Method and Apparatus

The experiment was conducted at an outdoor location located in the vicinity of the International Islamic University of Malaysia (IIUM) in Kuantan, Pahang (latitude N 3°50'42.47'' (3.84513°) and longitude of E 103°18'11.76'' (103.30327°)). The temperature data was recorded by using Advantech ADAMview data logger system at every 1-minute time span from 9:00 a.m. until 7:00 p.m. The K-type thermocouple with reading tolerance of ± 1.5 °C used to measure the temperature data was installed at multiple location across the system as shown in the Figure 3. The solar radiation and wind speed were measured using Apogee pyranometer (calibration uncertainty of 5 %) and hot wire anemometer, respectively. The air mass flowrate was set to be flowing through the collector at 0.004 kg/s for the entire experimental period. The experimental work was conducted in 2-phase namely, Phase 1 and Phase 2. The thermal performance of CMA-DPSAH integrated with thermal energy storage (Phase 1) was compared with the CMA-DPSAH without thermal energy storage (Phase 2) material inserted.
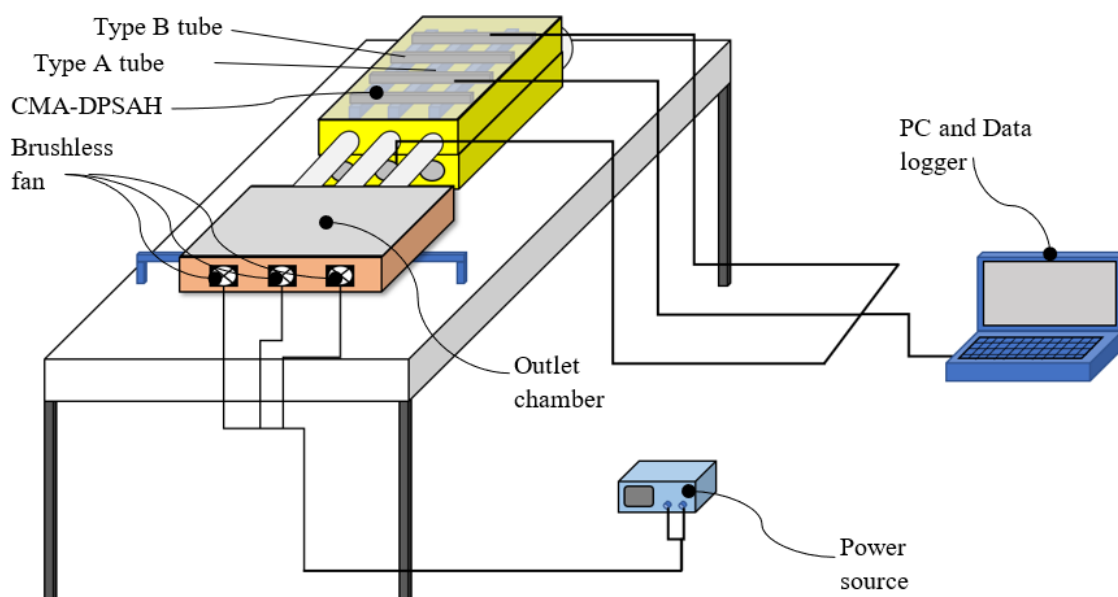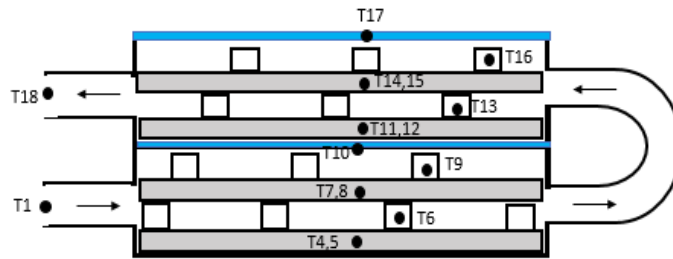

Fig. 2. Experimental setup used in this work

= thermocouple location:
T1 : Inlet temperature
T4,5 : Type B outer surface and inner (PCM) temperature, location 1
T6 : Type A outer surface temperature, location 1
T7,8 : Type B outer surface and inner (PCM) temperature, location 2
T9 : Type A outer surface temperature, location 2
T10 : Intermediate glazing temperature

T11,12 : Type B outer surface and inner (PCM) temperature, location 3
T13 : Type A outer surface temperature, location 3
T14,15 : Type B outer surface and inner (PCM) temperature, location 4
T16 : Type A outer surface temperature, location 4
T17 : Outer glazing temperature
T18: Outlet temperature

Fig. 3. Thermocouple positioning on respective tube and glazing

In order to evaluate the effectiveness of the thermal energy storage utilized in the CMA-DPSAH, the rate of charging and discharging were calculated based on the following expression [28]:

$$Heat\ Charging\ rate\quad = \frac{\Delta T_{Charge}}{\Delta t_{charge}} \tag{1}$$

$$Heat\ Discharging\ rate = \frac{\Delta T_{discharge}}{\Delta t_{discharge}} \tag{2}$$

The thermal efficiency of the collector during charging and discharging process was calculated based on the Eqs. (3) and (4), respectively [29].

$$\eta_{Charging} = \frac{Q_U + Q_S}{A_T I} \tag{3}$$

$$\eta_{Discharging} = \frac{Q_U}{Q_S} \tag{4}$$

where Q_U and Q_S are useful heat gained and heat stored which were given by Eqs. (5) and (6), as follows

$$Q_U = \dot{m} c_p (T_{out} - T_{in}) \tag{5}$$

$$Q_s = \frac{m_{pcm}}{\Delta t} c_{p,s} \Delta T_{pcm} \qquad T_{avg,pcm} < T_m$$

$$Q_s = \left(\frac{m_{pcm} L_{pcm}}{\Delta t} \right) \qquad T_{avg,pcm} = T_m \tag{6}$$

$$Q_s = \frac{m_{pcm}}{\Delta t} c_{p,l} \Delta T_{pcm} \qquad T_{avg,pcm} > T_m$$

where T_{pcm}, $T_{avg,pcm}$, T_m, $c_{p,s}$, $c_{p,l}$ and m_{pcm} are PCM temperature rise, average PCM temperature, solid phase, liquid phase specific heat of PCM and PCM mass, respectively. As for latent heat calculation, in which for the case of stored heat by the PCM, the sensible heat mode will be take

placed when the average PCM temperature, $T_{avg,pcm}$ is below or exceeding the melting temperature, T_m, otherwise the method will be latent heat [29-30].

2.2 Uncertainty Analysis

It is imperative to ensure the measurement of the parameters taken using the correct tool in order to produce the reliable data and to avoid error. This error might come from a various source such as human, measurement apparatus and environment of an experimental work. In this work, uncertainty analysis was conducted using the method available in the literature [31-32] based on the following expression:

$$W_R = \left[\left(\frac{\partial R}{\partial x_1} w_1 \right)^2 + \left(\frac{\partial R}{\partial x_2} w_2 \right)^2 + \cdots + \left(\frac{\partial R}{\partial x_n} w_n \right)^2 \right] \qquad (7)$$

In which the average percentage value of an uncertainty of each measured and calculated parameter were 1.52 % and 7.85 %; respectively.

3. Results and Discussion

The experimental work was conducted in between the month of April and May 2019 under the cloudy sunny day condition. Figure 4 show the solar radiation profile as a function of time starting from 9:00 a.m. until 7:00 p.m. for each phase of an experiment (Phase 1 experiment was measured on 16th of April 2018 and Phase 2 was measured on 16th of May 2018). As can be seen in the Figure 4, the solar radiation distribution of phase 1 having a stable profile with the weather slightly in better shape as compared to the condition of phase 2. During the phase 2, the weather condition in the morning was slightly cloudy with the condition becomes better as the day passes by. As expected, the highest solar radiation was recorded during the middle of the day for both cases with maximum value of 1017 W/m² and 944 W/m² for phase 1 and phase 2, respectively. At the time frame between 1:30 p.m. until 2:30 p.m.; phase 1 experiment experienced solar radiation drop about 89 W/m² while phase 2 experiment's solar radiation drop was 65 W/m². At the end of the experiment period which was at around 6:30 p.m., solar radiation for both phases approached zero.

Figure 5(a) and (b) shows the temperature profile for the aluminium tube and solar radiation as a function of time for both experiment phase 1 and phase 2. From the figure, there are two temperature envelop for first air passage (T4, T6, T7 & T9) and second air passage (T11, T13, T14 & T16) for each DPSAH-CMA used in phase 1 and phase 2 experiment. The temperature envelop of second air passage was higher than the one from first air passage due to the fact that the second air passage of DPSAH-CMA design was located at the top portion of the collector. As expected, the temperature of all aluminium tube component having a similar profile which reached at maximum value at 1:00 p.m. However, the temperature built-up for phase 1 experiment was slower as compared to the phase 2 due to the fact that the heat flux supplied during the charging process was utilized to melt the solid paraffin wax in the DPSAH-CMA in phase 1 experiment. We can conclude that during the radiation flux dropped, the solidification of the paraffin wax material helps to maintained the temperature of the tube without significant fluctuation due to thermal buffer created form the solidification of the paraffin wax. The evidence can be seen the plotted curve presented in Figure 5(a), where the flat temperature profile for phase 1 experiment was occur for about 30-minute.
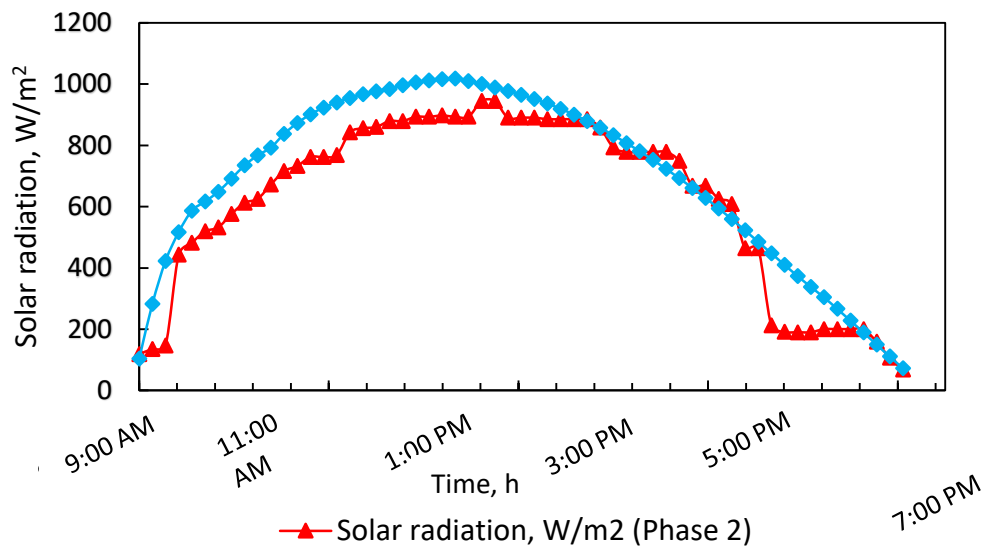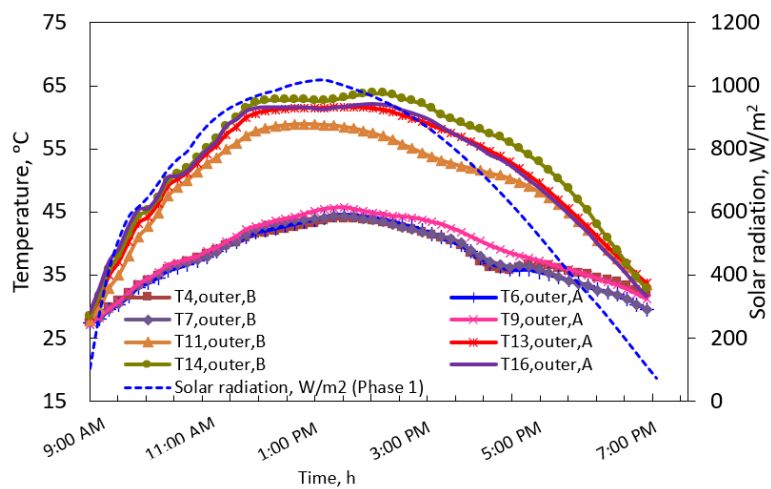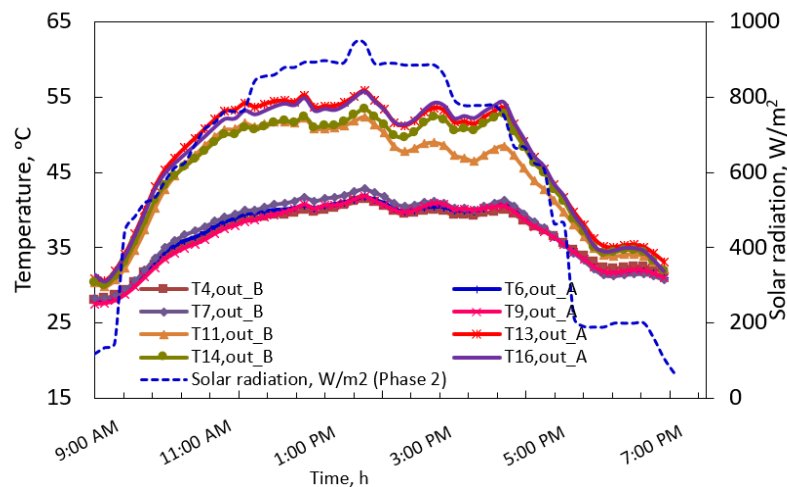
Fig. 4. Solar radiation distribution during phase 1 (CMA-DPSAH with PCM) and phase 2 (CMA-DPSAH without PCM) of the experiments

(a) Aluminum tube temperature profile (Phase 1)

(b) Aluminum tube temperature profile (Phase 2)

Fig. 5. Aluminum temperature profile for (a) Phase 1- with PCM and; (b) Phase 2- without PCM

In order to further enlighten this occasion, inlet and outlet temperature of each phase were plotted as a function of time as shown in Figure 6. The output temperature profile was increased gradually with the increase of inlet temperature and solar radiation as previously explained from the Figure 4. It is expected that the inlet and outlet temperature of phase 1 experiment was higher than the one of phase 2 experiment due to the slightly higher solar radiation. During this period, the temperature increases due to the sensible heat of the absorber material for each CMA-DPSAH used in the experiment. In the middle of the day, which was around 12:30 p.m. to 1:30 p.m., the latent heat of fusion started to take over for the CMA-DPSAH used in phase 1 (with PCM) as it is expected that all of the paraffin inside the tube was completely melted and absorbed the thermal energy from the solar radiation flux. For the sake of comparison on the performance between the two scenarios, the selected time range between 1:40 p.m. until 2:20 p.m. was selected in order to analyse the performance of each CMA-DPSAH's as highlighted in the purple dotted box, shown in the Figure 5.

During this specific time range, the radiation drop for phase 1 experiment was 58.28 W/m2 while the radiation drop for phase 2 experiment was only 4.70 W/m2. It can be seen that albeit part of the PCM was solidified during 40-minutes of solar radiation dropped, the amount of thermal energy released during the solidification was able to maintained the output temperature stability of the CMA-DPSAH during phase 1 experiment at discharge rate of 0.007 °C/min. In comparison with the case of experiment of phase 2, the discharge rate was calculated to be 0.096 °C/min even with the small amount of radiation drop. This observation suggests the properties of aluminium tube of having a higher heat diffusivity with a very minimal capability of storing the thermal energy received from the solar radiation flux.
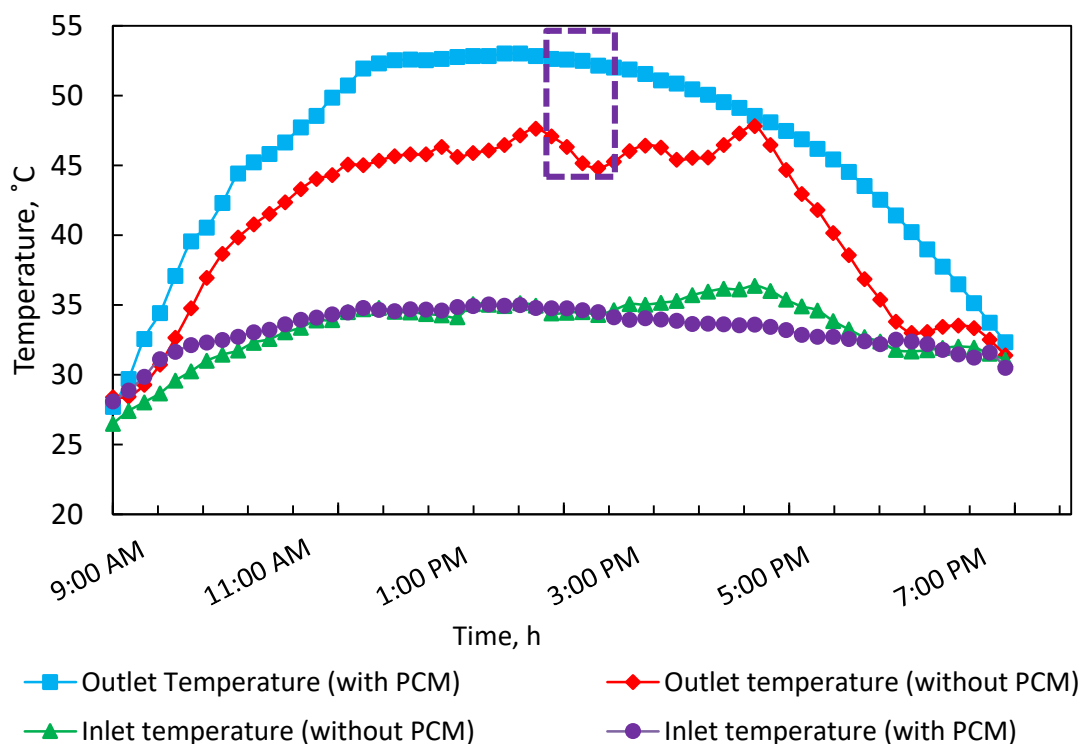

Fig. 6. Inlet and outlet temperature profile for configuration with PCM (Phase 1) and without PCM (Phase 2)

In order to evaluate the effectiveness of using PCM inside the absorber tube, the heat gain and temperature different for each phase were plotted and presented in Figure 7 with the interpretation of the result was based on the ambient temperature condition and the range of solar radiation during

the whole experimental period. During the phase 1 experiment, the ambient temperature was varied between 24.4 – 31.4 ˚C with the range of solar radiation of 103 – 1017 W/m². The paraffin wax not melted during the beginning of the experimental period and the output temperature increment was driven by the sensible heat produced by the thermal absorber and the heated solid paraffin wax. As the solar radiation flux reach at higher value in the middle of the day, the melted paraffin wax started to collect the heat flux until all of the paraffin wax were fully melted. As soon as the solar radiation drop, it is noticed that the temperature different profile maintained at higher side for about 30 minutes, due to the thermal buffer effect caused by the latent heat contribution from the solidifying of the paraffin wax. In comparison with phase 2 experiment, the ambient temperature was varied between 26.1 – 31 ˚C with solar radiation varied between 118 – 944 W/m² and the temperature different profile was fluctuate based on the fluctuation of the solar radiation. This was again due to the poor thermal storage capability of the aluminium tube thermal absorbers[33].

Heat gained by each collector was calculated using Eqs. (5) and (6) with the latent heat effect was taken into consideration for the phase 1 collector. As expected, the maximum energy gain by each collector was at a maximum value in the middle of the day with CMA-DPSAH with PCM (Phase 1) and CMA-DPSAH without PCM (Phase 2) maximum heat gain is 127 W and 89 W, respectively at around 1:40 p.m. The total heat gained by the collector with PCM was not only in the form of sensible heat from the absorber tube material itself, but also from the sensible heat (before the melting of the paraffin wax) and latent heat of the paraffin wax (during the freezing of the melted paraffin wax due to the decrement of radiation flux). It is concluded that, with the design of cross-matrix thermal absorber and integrating with PCM was not only capable to increase the heat transfer surface area and retaining the higher temperature of the absorber but also provide a much-improved useful heat into the flowing air.
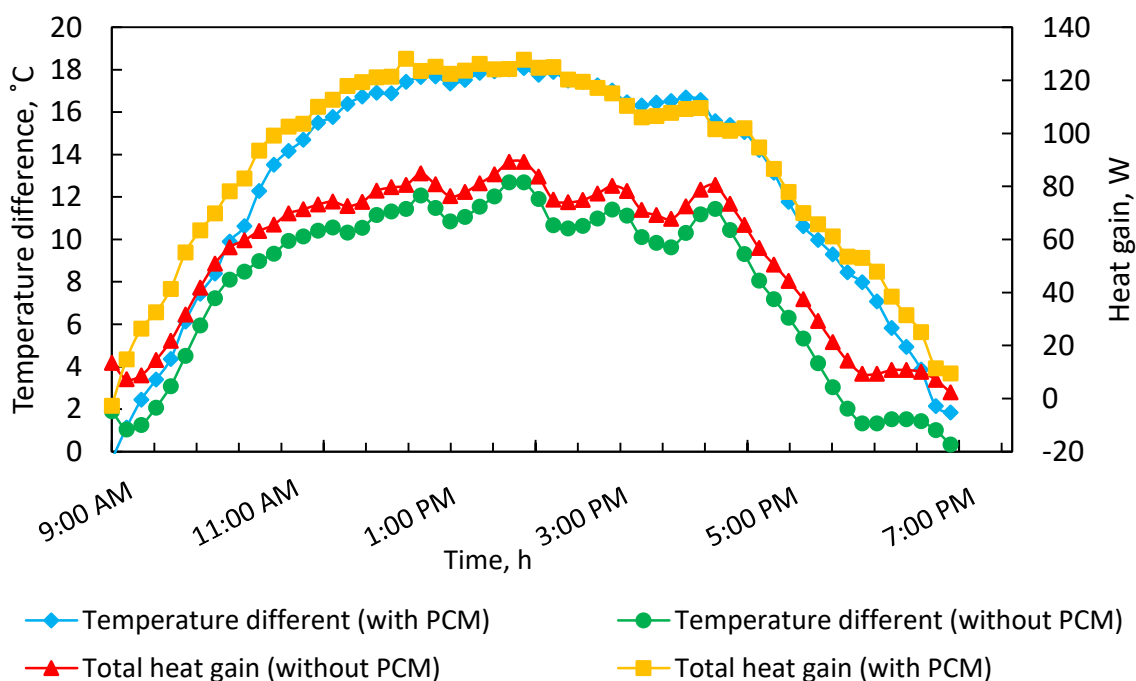

Fig. 7. Temperature difference and heat gain profile for each collector

To evaluate the effectiveness of the heat exchange between the absorber and the air flowing through it, the plot of output temperature as a function of average absorber temperature is presented in Figure 8. Based on the plot, it can be concluded that the output temperature varies

linearly with the average absorber temperature, with the mathematical correlation was presented for the air flow rate of 0.004 kg/s. This observation shows the good heat exchange rate between the flowing air and the cross-matrix thermal absorber.

Figure 9 present the instantaneous efficiency of both DPSAH-CMA for the mass flow rate of 0.004 kg/s. The instantaneous efficiency of DPSAH-CMA without PCM (phase 2) increase as the time passes by until the peak solar radiation flux with maximum range of 24-25 % and gradually decrease towards the end of the experimental hours.
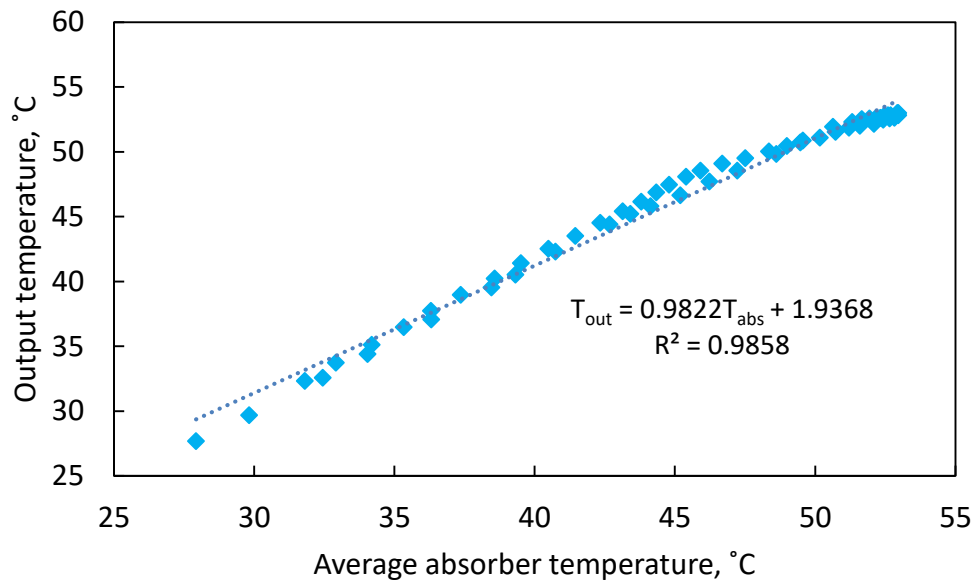

$$T_{out} = 0.9822T_{abs} + 1.9368$$
$$R^2 = 0.9858$$

Fig. 8. Output temperature of the DPSAH-CMA with PCM as a function of average absorber temperature

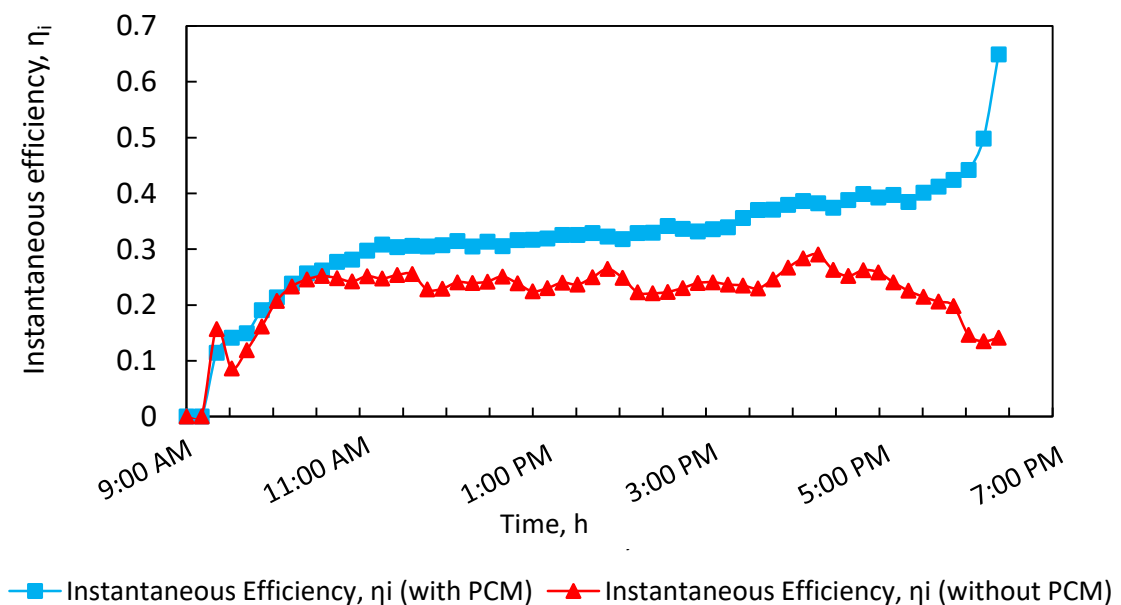Instantaneous Efficiency, η_i (with PCM) — Instantaneous Efficiency, η_i (without PCM)

Fig. 9. Instantaneous efficiency of each collector as a function of time

For the case of DPSAH-CMA with PCM (phase 1), the instantaneous efficiency increases with the increasing time, with the maximum range of instantaneous efficiency during the peak solar radiation flux of 32-34 %, and further increase to the maximum value toward the end of the experimental hours. This was due to the fact that during the low radiation flux, the air flowing through the collector under lower heat input in-terms of solar radiation flux, still be heated by the heat flux released from the paraffin wax during the solidification process. The instantaneous efficiency for CMA-DPSAH with PCM during the dropping of the radiation flux, which was significantly started at 3:00 p.m., was varied between 40 – 64 % whereas for CMA-DPSAH without PCM, the instantaneous efficiency was consistently lower by 17- 19 %. The higher value of thermal diffusivity of Aluminium making the temperature of the absorber tube drop much faster with the dropping of radiation flux [34].

4. Conclusions

The performance of DPSAH with PCM and without PCM were evaluated experimentally in the outdoor condition. Based on the result, several findings can be summarized as follows:

i.   The DPSAH-CMA with PCM (used in Phase 1 experiment) capable to sustained the useful heat during the solar radiation fluctuation. The average heat gain during 1 hour after radiation drop starting at around 1:00 p.m. was 124.96 W. Meanwhile the average heat gain for DPSAH-CMA without PCM (used in Phase 2 experiment) under the same condition was 96.51 W.

ii. With the incorporation of PCM, the calculated heat discharging rate for CMA-DPSAH with PCM was 4 times higher than the one without PCM due to thermal buffer as an effect from the latent heat produced by the solidification of the paraffin wax. The performance of CMA-DPSAH improved significantly with the incorporation of PCM especially in the condition where there is a fluctuation of solar radiation or during the off-sunshine period.

iii. The instantaneous efficiency of the CMA-DPSAH with the PCM was consistently higher than the one without PCM by 17- 19 % with the CMA-DPSAH with PCM gaining more energy that can be transferred to the flowing air. This condition was significant after the solar radiation flux started to drop (from 3:00 p.m. onwards).

Acknowledgement

References
[1]   Kannan, Nadarajah, and Divagar Vakeesan. "Solar energy for future world:-A review." *Renewable and Sustainable Energy Reviews* 62 (2016): 1092-1105.
https://doi.org/10.1016/j.rser.2016.05.022

[2]   Mahmood, A. J., L. B. Y. Aldabbagh, and F. Egelioglu. "Investigation of single and double pass solar air heater with transverse fins and a package wire mesh layer." *Energy conversion and management* 89 (2015): 599-607.
https://doi.org/10.1016/j.enconman.2014.10.028

[3]   A. J. Mahmood and L. B. Y. Aldabbagh. "Double Pass Solar Air Heater with Transvers Fins and without Absorber Plate. " *Int. J. Mech. Aerospace, Ind. Mechatron. Manuf. Eng.*, 7, no. 6 (2013): 1293–1298.

[4]   Wong, Rudy JD, Manar Al-Jethelah, Soroush Ebadi, Ashutosh Singh, and Shohel Mahmud. "Investigation of phase change materials integrated with fin-tube baseboard convector for space heating." *Energy and Buildings* 187 (2019): 241-256.
https://doi.org/10.1016/j.enbuild.2019.02.005

[5]   Jamal-Abad, Milad Tajik, Seyfolah Saedodin, and Mohammad Aminy. "Heat transfer in concentrated solar air-heaters filled with a porous medium with radiation effects: A perturbation solution." *Renewable Energy* 91 (2016): 147-154.

https://doi.org/10.1016/j.renene.2016.01.050

[6]   Zhou, Dan, and C. Y. Zhao. "Experimental investigations on heat transfer in phase change materials (PCMs) embedded in porous materials." *Applied Thermal Engineering* 31, no. 5 (2011): 970-977.
https://doi.org/10.1016/j.applthermaleng.2010.11.022

[7]   Dehghan, Maziar, Yousef Rahmani, Davood Domiri Ganji, Seyfollah Saedodin, Mohammad Sadegh Valipour, and Saman Rashidi. "Convection–radiation heat transfer in solar heat exchangers filled with a porous medium: homotopy perturbation method versus numerical analysis." *Renewable Energy* 74 (2015): 448-455.
https://doi.org/10.1016/j.renene.2014.08.044

[8]   Hans, V. S., R. S. Gill, and Sukhmeet Singh. "Heat transfer and friction factor correlations for a solar air heater duct roughened artificially with broken arc ribs." *Experimental Thermal and Fluid Science* 80 (2017): 77-89.
https://doi.org/10.1016/j.expthermflusci.2016.07.022

[9]   Ravi, Ravi Kant, and R. P. Saini. "Experimental investigation on performance of a double pass artificial roughened solar air heater duct having roughness elements of the combination of discrete multi V shaped and staggered ribs." *Energy* 116 (2016): 507-516.
https://doi.org/10.1016/j.energy.2016.09.138

[10]   Ravi, Ravi Kant, and R. P. Saini. "Effect of roughness elements on thermal and thermohydraulic performance of double pass solar air heater duct having discrete multi V-shaped and staggered rib roughness on both sides of the absorber plate." *Experimental Heat Transfer* 31, no. 1 (2018): 47-67.
https://doi.org/10.1080/08916152.2017.1350217

[11]   Salih, Mothana M. Mohamed, Omar Rafae Alomar, Firas Aziz Ali, and Hareth Maher Abd. "An experimental investigation of a double pass solar air heater performance: A comparison between natural and forced air circulation processes." *Solar Energy* 193 (2019): 184-194.
https://doi.org/10.1016/j.solener.2019.09.060

[12]   Abo-Elfadl, Saleh, Hamdy Hassan, and M. F. El-Dosoky. "Study of the performance of double pass solar air heater of a new designed absorber: An experimental work." *Solar Energy* 198 (2020): 479-489.
https://doi.org/10.1016/j.solener.2020.01.091

[13]   Kalaiarasi, G., R. Velraj, and Muthusamy V. Swami. "Experimental energy and exergy analysis of a flat plate solar air heater with a new design of integrated sensible heat storage." *Energy* 111 (2016): 609-619.
https://doi.org/10.1016/j.energy.2016.05.110

[14]   Singh, Sameer Kumar. "PERFORMANCE ANALYSIS OF SOLAR AIR HEATER WITH PHASE CHANGE MATERIAL." (2017).

[15]   Kalaiarasi, G., R. Velraj, M. N. Vanjeswaran, and N. Ganesh Pandian. "Experimental analysis and comparison of flat plate solar air heater with and without integrated sensible heat storage." *Renewable Energy* 150 (2020): 255-265.
https://doi.org/10.1016/j.renene.2019.12.116

[16]   Asgharian, H., and E. Baniasadi. "A review on modeling and simulation of solar energy storage systems based on phase change materials." *Journal of Energy Storage* 21 (2019): 186-201.
https://doi.org/10.1016/j.est.2018.11.025

[17]   Sarbu, Ioan, and Calin Sebarchievici. "A comprehensive review of thermal energy storage." *Sustainability* 10, no. 1 (2018): 191.
https://doi.org/10.3390/su10010191

[18]   Khan, Mohammed Mumtaz A., Nasiru I. Ibrahim, I. M. Mahbubul, Hafiz Muhammad Ali, R. Saidur, and Fahad A. Al-Sulaiman. "Evaluation of solar collector designs with integrated latent heat thermal energy storage: a review." *Solar Energy* 166 (2018): 334-350.
https://doi.org/10.1016/j.solener.2018.03.014

[19]   Haldorai, Sivarathinamoorthy, Sureshkannan Gurusamy, and Maruthaiyan Pradhapraj. "A review on thermal energy storage systems in solar air heaters." *International Journal of Energy Research* 43, no. 12 (2019): 6061-6077.
https://doi.org/10.1002/er.4379

[20]   Bouadila, Salwa, Sami Kooli, Mariem Lazaar, Safa Skouri, and Abdelhamid Farhat. "Performance of a new solar air heater with packed-bed latent storage energy for nocturnal use." *Applied Energy* 110 (2013): 267-275.
https://doi.org/10.1016/j.apenergy.2013.04.062

[21]   Salih, Salah M., Jalal M. Jalil, and Saleh E. Najim. "Experimental and numerical analysis of double-pass solar air heater utilizing multiple capsules PCM." *Renewable Energy* 143 (2019): 1053-1066.
https://doi.org/10.1016/j.renene.2019.05.050

[22]   Baig, Wajahat, and Hafiz Muhammad Ali. "An experimental investigation of performance of a double pass solar air heater with foam aluminum thermal storage medium." *Case Studies in Thermal Engineering* 14 (2019): 100440.
https://doi.org/10.1016/j.csite.2019.100440

[23]   Saxena, Abhishek, Prashant Verma, Ghanshyam Srivastava, and Nand Kishore. "Design and thermal performance evaluation of an air heater with low cost thermal energy storage." *Applied Thermal Engineering* 167 (2020):

114768.
https://doi.org/10.1016/j.applthermaleng.2019.114768

[24] Raj, A. K., M. Srinivas, and S. Jayaraj. "A cost-effective method to improve the performance of solar air heaters using discrete macro-encapsulated PCM capsules for drying applications." *Applied Thermal Engineering* 146 (2019): 910-920.
https://doi.org/10.1016/j.applthermaleng.2018.10.055

[25] Sharol, A. F., A. A. Razak, Z. A. A. Majid, M. A. A. Azmi, and M. A. S. M. Tarminzi. "Performance of force circulation cross-matrix absorber solar heater integrated with latent heat energy storage material." In *IOP Conference Series: Materials Science and Engineering*, vol. 469, no. 1, p. 012107. IOP Publishing, 2019.
https://doi.org/10.1088/1757-899X/469/1/012107

[26] Razak, A. A., Z. A. A. Majid, F. Basrawi, A. F. Sharol, Mohd Hafidz Ruslan, and Kamaruzzaman Sopian. "A performance and technoeconomic study of different geometrical designs of compact single-pass cross-matrix solar air collector with square-tube absorbers." *Solar Energy* 178 (2019): 314-330.
https://doi.org/10.1016/j.solener.2018.12.010

[27] Enibe, S. O. "Thermal analysis of a natural circulation solar air heater with phase change material energy storage." *Renewable Energy* 28, no. 14 (2003): 2269-2299.
https://doi.org/10.1016/S0960-1481(03)00071-5

[28] Sharol, Ahmad Fadzil, Amir Abdul Razak, Zafri Azran Abdul Majid, and Ahmad Fudholi. "Experimental study on performance of square tube absorber with phase change material." *International Journal of Energy Research* 44, no. 2 (2020): 1000-1011.
https://doi.org/10.1002/er.4971

[29] Kabeel, A. E., A. Khalil, S. M. Shalaby, and M. E. Zayed. "Improvement of thermal performance of the finned plate solar air heater by using latent heat thermal storage." *Applied Thermal Engineering* 123 (2017): 546-553.
https://doi.org/10.1016/j.applthermaleng.2017.05.126

[30] El-Sebaii, A. A., A. A. Al-Ghamdi, F. S. Al-Hazmi, and Adel S. Faidah. "Thermal performance of a single basin solar still with PCM as a storage medium." *Applied Energy* 86, no. 7-8 (2009): 1187-1195.
https://doi.org/10.1016/j.apenergy.2008.10.014

[31] Yahya, M., Ahmad Fudholi, and Kamaruzzaman Sopian. "Energy and exergy analyses of solar-assisted fluidized bed drying integrated with biomass furnace." *Renewable Energy* 105 (2017): 22-29.
https://doi.org/10.1016/j.renene.2016.12.049

[32] Şevik, Seyfi. "Experimental investigation of a new design solar-heat pump dryer under the different climatic conditions and drying behavior of selected products." *Solar Energy* 105 (2014): 190-205.
https://doi.org/10.1016/j.solener.2014.03.037

[33] Majid, Z. A. A., A. A. Razak, Mohd Hafidz Ruslan, and Kamaruzzaman Sopian. "Characteristics of solar thermal absorber materials for cross absorber design in solar air collector." *International Journal of Automotive and Mechanical Engineering* 11 (2015): 2582-2590.
https://doi.org/10.15282/ijame.11.2015.36.0217

[34] M. B. Y. Cengel. *Thermodynamics-An engineering approaches*, 5th ed. Mc Graw-Hill, 2010.